

Mechanisms of Protein Crystal Growth: An Atomic Force Microscopy Study of Canavalin Crystallization

T. A. Land,¹ A. J. Malkin,² Yu.G Kuznetsov,² A. McPherson,² and J. J. De Yoreo¹

¹*Department of Chemistry and Materials Science, Lawrence Livermore National Laboratory, Livermore, California 94550*

²*Department of Biochemistry, University of California at Riverside, Riverside, California 92521*

(Received 2 May 1995)

In situ atomic force microscopy has been used to investigate step dynamics and surface evolution during the growth of single crystals of canavalin, a protein with a well known structure. Growth occurs by step flow on complex dislocation hillocks, and involves the formation and incorporation of small, mobile molecular clusters. Defects in the form of hollow channels are observed and persist over growth times of several days. The results are used to establish a physical picture of the growth mechanism, and estimate the values of the free energy of the step edge, α , and the kinetic coefficient, β .

PACS numbers: 87.15.Da, 61.16.Ch, 61.50.Cj, 68.35.Bs

The crucial functions of biological systems are governed by macromolecules, such as proteins and nucleic acids, whose specific roles are in turn defined by their structures. Experimentally, macromolecular structure is determined using x-ray crystallographic methods [1,2] which require large, uniform single crystals of the macromolecules. However, crystallization of proteins and other biological molecules is highly problematic, to such an extent that it has become the rate limiting step in most structure analyses. This is true, in large part, because little is known of the growth mechanisms, the events leading to nucleation, or the fundamental thermodynamic and kinetic parameters that determine growth rates and surface morphologies. Less still is understood about the incorporation of defects, the forces responsible for the orientation and bonding of molecules in the lattice, or the role of transport processes, a factor of particular relevance to studies of the phenomenon in microgravity environments [3,4]. A more detailed and comprehensive understanding of all these questions is required if the current obstacles to macromolecular crystal growth are to be overcome.

Beyond this important practical consideration is the realization that the slow growth kinetics and large molecular diameters of biological molecules make macromolecular crystals ideal systems for the investigation of homoepitaxy in real time using scanned probe microscopies. While real time experiments have been performed using scanning tunneling microscopy on both metal [5] and semiconductor [6,7] surfaces, limited progress has been made due to the rapid kinetics of atomic motion on such surfaces and the influence of the voltage at the tip on that motion. In addition, these studies have focused on adatom motion in systems with low surface coverage, rather than the advance of the crystal surface itself. Following the demonstration of atomic force microscopy (AFM) as a useful tool for investigating both solution crystal growth [8] and biological structures [9], Durbin and Carlson [10] successfully used AFM to monitor the growth of single crystals of the protein lysozyme. Their observations were

consistent with the general physical picture of growth first developed for inorganic systems by Burton, Cabrera, and Frank [11]. In that model, growth from solution occurs by step-flow on steps generated by screw dislocations of two-dimensional (2D) nucleation through incorporation of monomers at the step edges, either directly from solution or following adsorption onto and diffusion across the terraces. During dislocation controlled growth, the dislocation with the largest Burgers vector provides the dominant growth source.

Here we report the results of *in situ* atomic force microscopy on single crystals of the protein canavalin, which reveal a somewhat different picture of growth. The results show that the growth of canavalin crystals occurs on complex vicinal hillocks formed by multiple, independently acting screw dislocation sources. While growth occurs at monomolecular steps, on the terraces of these steps we observe the continual formation of a large number of molecular clusters with diameters of less than ten molecules. These clusters exist in a state of dynamic equilibrium undergoing dissolution, migration, and incorporation at step edges as the steps move across the terraces. From the roughness of the steps, we estimate the free energy of the step edge per unit step height α , and from the speed of the steps, we calculate the kinetic coefficient for step motion β . We find further that canavalin crystals contain defects in the form of hollow channels as large as $2 \mu\text{m}$ diameter. Some are formed at the dislocation cores, but other are not connected with screw dislocations and persist for growth periods of many days. We argue that these holes are caused by incorporation of foreign particles adsorbed onto the surface. Finally, we show that the growth rate of canavalin is enhanced in the region scanned by the AFM tip, indicating that, under typical conditions, canavalin crystal growth is limited by solute transport to the surface.

Canavalin ($M_r = 1.47 \times 10^5$ Da), which is the major storage protein of the jack bean and exhibits properties common to many storage proteins, was chosen for

this study because its structure has been accurately determined, and it is easily and reproducibly crystallized. Stock aqueous solutions of canavalin with a concentration of 38 mg/ml were prepared as described previously [12]. Crystals of canavalin were nucleated on etched glass substrates within the sealed fluid cell of a Digital Nanoscope III atomic force microscope whose basic operation has been described elsewhere [8]. After mixing of the stock solution with the precipitant Dulcecco-phosphate buffered saline ($2 \times$ DPBS) in the ratio of 1:1.5, the resulting solution was injected into the cell and allowed to incubate until crystals of 10–500 μm in size were observed. Images were collected in contact mode, using cantilevers with nominal force constants of 0.06 to 0.38 $\text{N}\cdot\text{m}^{-1}$. Forces of <0.1 to 0.5 nN were applied during imaging. With forces in this range, our experiments on numerous crystalline systems have shown that crystals can be imaged during growth without destruction of steps.

Canavalin crystallizes in many forms, depending on the crystallization conditions [13]. We observed the growth on the {100} face of rhombohedral canavalin crystals of space group $R3$. The structure of this crystal form, as well as that of the canavalin trimer which occupies the lattice sites, is shown in Fig. 1(a) and 1(b). The canavalin trimer forms a three-sided ring with an outside diameter of 8.6–8.8 nm, an inside diameter 1.8 nm, and a thickness of 3.5–4.0 nm. As Fig. 1(b) shows, in the rhombohedral structure, these rings are canted out of the {100} plane by an angle of 29° . The unit cell dimensions are

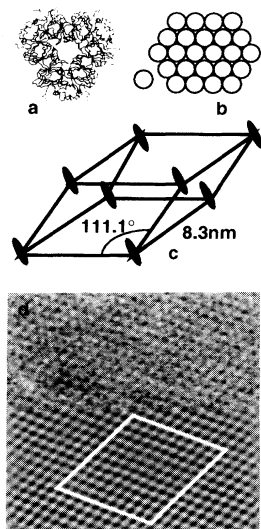


FIG. 1. (a) Structure of the canavalin trimer. (b) Example of a possible stable arrangement of a molecule in a 2D cluster with hexagonal packing. Addition of single molecules reduces stability. (c) The $R3$ rhombohedral crystal showing the orientation of the trimer rings with respect to the {100} plane. (d) A 250×250 nm AFM image of the canavalin surface before (upper) and after (lower) Fourier transform filtering. The dashed rhombus corresponds to ten unit cells.

$a = b = c = 8.3$ nm, with $\alpha = \beta = \gamma = 111.1^\circ$. The resulting distance between the {100} planes is 7.4 nm. An AFM image of the canavalin surface is shown in Fig. 1(d) in raw form, and after filtering, using the Fourier transform. The rhombohedral structure is seen clearly, and the measured lattice spacing and angles agree with the crystallographic data for this structure [13].

Growth of canavalin crystals was observed to occur at steps on complex vicinal hillocks, generated by multiple screw dislocation sources. The step heights were 7.0 ± 0.4 nm, showing that the surface advances on single trimer height steps. Figure 2 is a series of sequential images showing the evolution of a dislocation hillock on a 50 μm crystal. This hillock was the only growth source on the crystal and consisted of seven separate dislocation sources, generating a total of eight steps. Each source acted independently of the others in generating steps which merged to form the overall growth source. In contrast to the picture of growth described in the introduction, no single dislocation source was dominant, regardless of the size of the Burgers vector.

While dislocations provided the step sources, the formation and incorporation of small clusters was also an important step in the growth process. As is evident from Fig. 2, the terraces contain many small clusters. Figure 3 is a series of sequential images which show how these clusters interact with the advancing step and how the clusters distribution evolves with time. While some of the clusters desorb or dissolve on the time scale of imaging, many are stable and have low mobility. The clusters are incorporated into the advancing steps and thus provide a significant fraction of the molecules in the crystal. Little or no coalescence of adjacent clusters is observed, nor do the larger clusters grow with time. In fact, the images of the clusters are of nearly uniform size, measuring 70–90 nm and 35–50 nm in the fast and slow scan directions, respectively, and 3.9 nm in height. The measured cluster height suggests that the clusters consist of individual trimers lying flat on the {100} surface, rather than at the cant angle of the bulk trimers. However, the small size of the clusters precludes resolution of their true size, shape, or internal structure, and we can neither distinguish between amorphous and ordered packing nor determine of what multiple of canavalin molecules the clusters are comprised.

While distortion in the fast scan direction is likely for weakly bound objects on the surface, the measured dimension in the slow scan direction should be considerably less distorted. If these clusters are ordered, then the size range in this direction is no larger than that of hexagonally packed clusters of canavalin trimers with the first few rings filled as shown in Fig. 1(c). Recently, Rosenfeld *et al.* [14] reported that, under certain conditions, the growth of Pt(111) surfaces is characterized by the formation of small Pt clusters of nearly uniform size which are stable against both growth and decomposition. By consid-

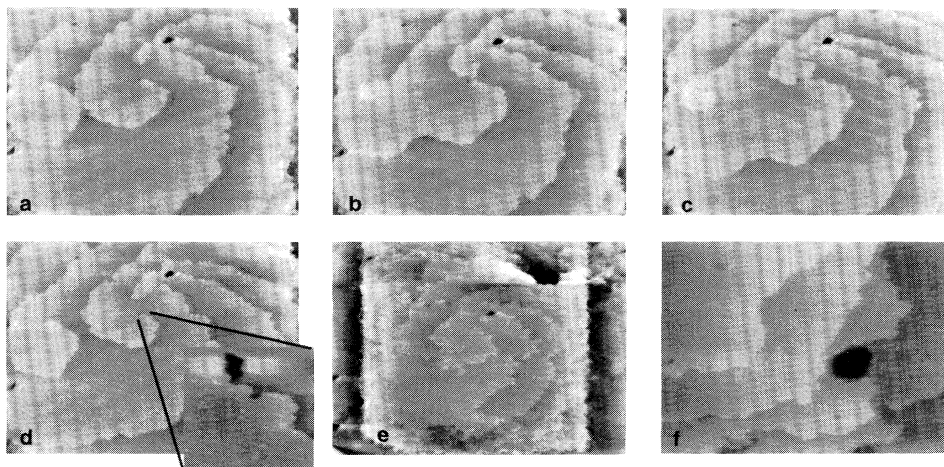


FIG. 2. (a)–(d) Sequence of $22.5 \times 17.1 \mu\text{m}$ images, separated by 86 s intervals, showing the evolution of growth spirals on canavalin. A dislocation source with a Burgers vector of two unit steps lies out of the field of view to the upper left and is visible in (e), a larger area ($27.4 \times 20.8 \mu\text{m}$) image showing the effect of scanning on growth. Examples of holes in canavalin crystals showing [inset to (d)] a $1.3 \times 1.3 \mu\text{m}$ image of a hollow dislocation core, and (f) a $6.0 \times 4.0 \mu\text{m}$ image of a channel not connected with a screw dislocation. See also Fig. 2(e).

ering the bond distribution of small clusters, they showed that those of a particular size, such as heptamers and decamers, should be favored. We suggest that similar energetic constraints are controlling the size of the canavalin clusters.

The fundamental growth parameters α , the free energy of the step edge per unit step height, and β , the kinetic coefficient for step motion, can be estimated from these AFM results. The relationship between α and r_c , the critical radius of curvature for an island or step, is given by [11]

$$r_c = \omega \alpha / kT\sigma, \quad (1)$$

where ω is the specific molecular volume and is equal to $4.1 \times 10^{-19} \text{cm}^3$ in rhombohedral canavalin, k is Boltzmann's constant, T is the temperature, and σ is the relative supersaturation. The value of r_c is bounded by the maximum curvature of the steps which, based on a large number of measurements of small capes (any convex portion of a step) on the step edges, is $95 \pm 28 \text{nm}$. For a typical supersaturation used in the experiments ($\sigma = 0.6$), we find that $\alpha < 0.6 \text{erg/cm}^2$. This is one to three orders of magnitude smaller than in inorganic systems [15] and reflects the high solvent content (30%–90%) of macromolecular crystals. Due to nearly equivalent environments in the solid and the solution, the amount of work required to create surface states can be expected to be lower in these systems.

The kinetic coefficient β is defined by the relationship [16]

$$v = \omega \beta (c - c_e), \quad (2)$$

where v is the step velocity, and c and c_e are the actual and equilibrium concentrations, respectively, of canavalin trimers in the solution. Step speeds were about 10^{-6}cm/s for $c = 1.2 \times 10^{16} \text{cm}^{-3}$ and $c_e = 0.65 \times$

10^{16}cm^{-3} , from which we calculate a kinetic coefficient for canavalin of 10^{-5} to 10^{-4}cm s^{-1} which is similar to that found for crystals of the satellite tobacco mosaic virus [17]. The kinetic coefficient itself is a measure of the kinetics of adsorption, diffusion, and incorporation, with the rate limiting step dominating the value of β . A typical value of β for inorganic crystals such as KH_2PO_4 is on the order of 10^{-2} to 10^{-1}cm s^{-1} . Thus the kinetic coefficient of elementary steps is about three orders of magnitude smaller in crystals of biological macromolecules than in inorganic crystals. The potential sources for the low value of β in these macromolecular systems include a large barrier to adsorption (shedding of the hydration sphere), low surface diffusivity, and a low probability that an incoming molecule has the proper orientation for incorporation into the crystal.

Through thermodynamic considerations of the effects of strain on crystal stability, Frank [18] and other [19,20] showed that, for sufficiently large Burgers vectors, a growth spiral should contain a hollow core. De Yoreo, Land, and Dair [21] found that the sizes of dislocation cores in KH_2PO_4 were in agreement with these theoretical predictions. We observed a number of holes in the surface of canavalin which persisted over growth times of several days to form hollow channels (see Fig. 2). A number of these holes were the source regions for screw dislocations, showing for the first time that macromolecular crystals also form hollow dislocation cores. However, the diameters varied with time and, between sources, with equal Burgers vectors. Furthermore, a number of holes were not connected with dislocations, as is seen in Figs. 2(e) and 2(f). We suggest that these holes are generally caused by incorporation of micron-size foreign particles and have observed this process directly on canavalin as well as on crystals of the satellite tobacco mosaic virus

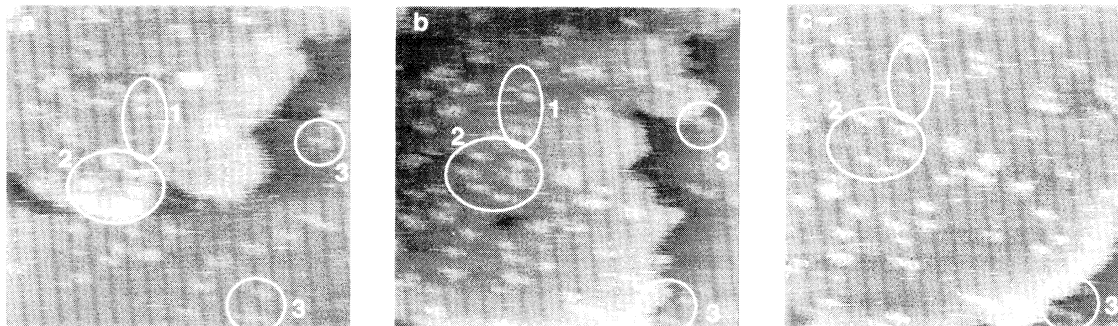


FIG. 3. Sequence of 900×900 nm images collected at times of: (a) 0, (b) 50.3 s and (c) 100.6 s showing the interaction of small clusters with a single step on the surface of canavalin. Circled areas show examples of clusters which (1) dissolve, (2) remain intact, and (3) are incorporated at step edges in subsequent images. The apparent irregular motion of the step is an artifact of the collection scheme. When an upward scan is followed by a downward scan as in (a) and (b), the portion of the step in the lower part of the image appears to advance farther than that in the upper part.

[17]. Following inclusion of a foreign particle, the site of incorporation becomes a hollow channel of the same size as the particle. This process was reported by Durbin [10] and is described in detail by Malkin *et al.* [17].

Finally, we found that the growth rate of canavalin was enhanced in the area scanned by the AFM tip. Upon increasing the scan size, the steps that had been generated within the scanned region were found to be bunched up at the edges, as shown in Fig. 2(e). This effect was not observed in other systems [17], and shows that mixing of the otherwise stagnant solution by the AFM tip near the crystal increases the growth rate. Figure 3 shows that this effect is clearly not caused by dislodging or reorientation of clusters and so must be a result of enhanced delivery of solute to the steps, either through bulk mixing or through mixing of a boundary layer. This result indicates that, under typical growth conditions, canavalin crystallization is limited by diffusion.

This work was performed under the auspices of the division of Materials Science, U.S. Department of Energy, and Lawrence Livermore National Laboratory, under contract No. W-7405-ENG48 and was supported by a grant from NASA.

[1] A. McPherson, *Sci. Am.* **260**, No. 3 62 (1989).

[2] C. Branden and J. Tooze, *Introduction to Protein Science* (Garland Publishing Inc., New York, 1991).

[3] L.J. Delucas *et al.* *Science* **246**, 651 (1989).

[4] J. Day and A. McPherson, *Protein Sci.* **1**, 254 (1992).

[5] S.J. Stranick, M.M. Kamna, and P.S. Weiss, *Science* **266**, 99 (1994).

[6] N. Kitamura, M.G. Lagally, and M.B. Webb, *Phys. Rev. Lett.* **71**, 2082 (1993).

[7] E. Ganz, S.K. Theiss, I.-S. Hwang, and J. Golovchenko, *Phys. Rev. Lett.* **68**, 1567 (1992).

[8] A.J. Gratz, S. Manne, and P.K. Hansma, *Science* **251**, 1343 (1991).

[9] P.K. Hansma, V.B. Elings, O. Marti, and C.E. Bracker, *Science* **242**, 209 (1988).

[10] S.D. Durbin and W.E. Carlson, *J. Cryst. Growth* **122**, 71 (1992); S.D. Durbin, *J. Phys. D.* **26**, B128 (1993).

[11] W.K. Burton, N. Cabrera, and F.C. Frank, *Philos. Trans. R. Soc. London A* **243**, 299 (1951).

[12] S.C. Smith, S. Johnson, J. Andrews, and A. McPherson, *Plant Physiol.* **70**, 1199 (1982).

[13] T.-P. Ko, J.D. Ng, J. Day, A. Greenwood, and A. McPherson, *Acta Crystallogr. Sect. D* **D49**, 478 (1993).

[14] G. Rosenfeld, A.F. Becker, B. Poelsema, L.K. Verheij, and G. Comsa, *Phys. Rev. Lett.* **69**, 917 (1992).

[15] O. Söhnel, *J. Cryst. Growth* **57**, 101 (1982).

[16] A.A. Chernov, *Sov. Phys. Usp.* **4**, 116 (1961).

[17] A.J. Malkin, T.A. Land, Yu.G. Kutznesov, A. McPherson, and J.J. De Yoreo, *Phys. Rev. Lett.* **75**, 2778 (1995).

[18] F.C. Frank, *Acta Crystallogr.* **4**, 497 (1951).

[19] N. Cabrera and M.M. Levine, *Philos. Mag.* **1**, 450 (1956).

[20] B. Van der Hoek, J.P. Van der Eerden, and P. Bennema, *J. Cryst. Growth* **56**, 621 (1982).

[21] J.J. De Yoreo, T.A. Land, and B.J. Dair, *Phys. Rev. Lett.* **73**, 838 (1994).

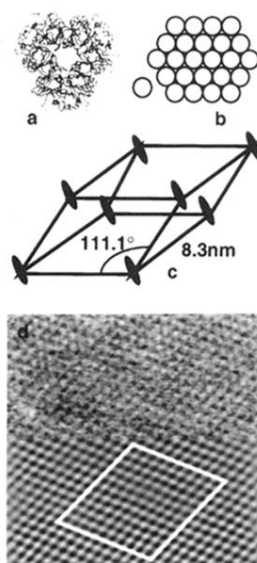


FIG. 1. (a) Structure of the canavalin trimer. (b) Example of a possible stable arrangement of a molecule in a 2D cluster with hexagonal packing. Addition of single molecules reduces stability. (c) The $R3$ rhombohedral crystal showing the orientation of the trimer rings with respect to the $\{100\}$ plane. (d) A 250×250 nm AFM image of the canavalin surface before (upper) and after (lower) Fourier transform filtering. The dashed rhombus corresponds to ten unit cells.

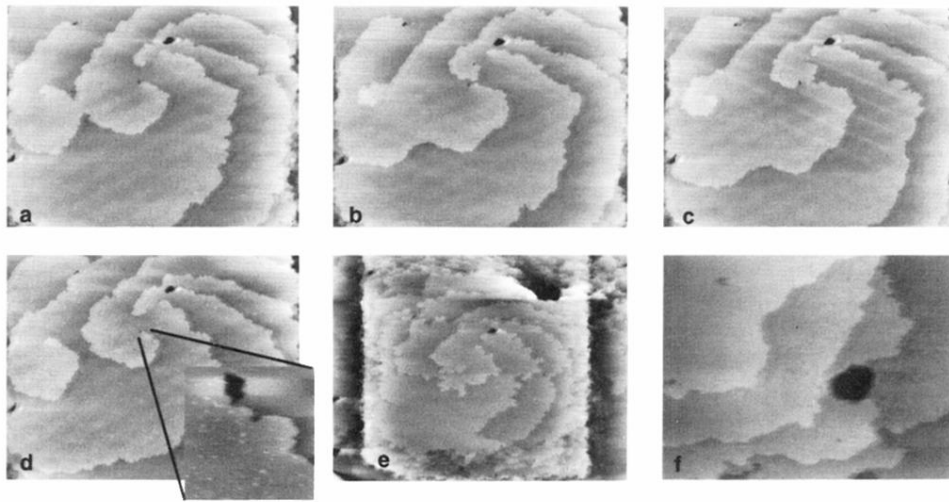


FIG. 2. (a)–(d) Sequence of $22.5 \times 17.1 \mu\text{m}$ images, separated by 86 s intervals, showing the evolution of growth spirals on canavalin. A dislocation source with a Burgers vector of two unit steps lies out of the field of view to the upper left and is visible in (e), a larger area ($27.4 \times 20.8 \mu\text{m}$) image showing the effect of scanning on growth. Examples of holes in canavalin crystals showing [inset to (d)] a $1.3 \times 1.3 \mu\text{m}$ image of a hollow dislocation core, and (f) a $6.0 \times 4.0 \mu\text{m}$ image of a channel not connected with a screw dislocation. See also Fig. 2(e).

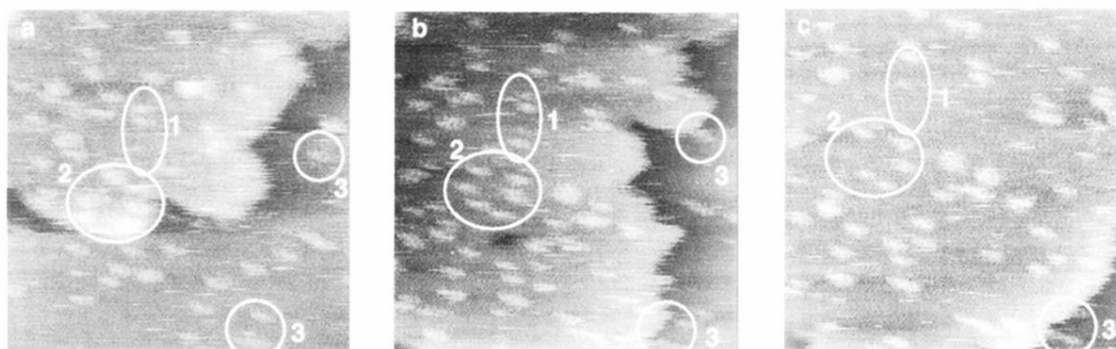


FIG. 3. Sequence of 900×900 nm images collected at times of: (a) 0, (b) 50.3 s and (c) 100.6 s showing the interaction of small clusters with a single step on the surface of canavalin. Circled areas show examples of clusters which (1) dissolve, (2) remain intact, and (3) are incorporated at step edges in subsequent images. The apparent irregular motion of the step is an artifact of the collection scheme. When an upward scan is followed by a downward scan as in (a) and (b), the portion of the step in the lower part of the image appears to advance farther than that in the upper part.